Available online at www.sciencedirect.com
ScienceDirect
Polyhedron 26 (2007) 5432–5440
POLYHEDRON
www.elsevier.com/locate/poly

Synthesis and characterization of novel 4-nitro-2-(octyloxy)phenoxy substituted symmetrical and unsymmetrical Zn(II), Co(II) and Lu(III) phthalocyanines

Duygu Kulaç [a], Mustafa Bulut [a], Ahmet Altındal [b], Ali Rıza Özkaya [a], Bekir Salih [c], Özer Bekaroğlu [d,*]

[a] Department of Chemistry, Marmara University, Göztepe 34722, Istanbul, Turkey
[b] Department of Physics, Marmara University, Göztepe 34722, Istanbul, Turkey
[c] Department of Chemistry, University of Hacettepe, 06532 Ankara, Turkey
[d] Department of Chemistry, Technical University of Istanbul, 34469 Maslak, Istanbul, Turkey

Received 10 May 2007; accepted 8 August 2007
Available online 27 September 2007

Abstract

Compounds **3** and **4** have been prepared by the reaction of 4-nitrocatechol **1** and 4-nitrophthalonitrile **2** by a common method, aromatic nucleophilic subtitution of the nitro group in 4-nitrophthalonitrile. Starting from **4** and 1-bromooctane, their alkylation reaction gave compound **5**. Zn(II) **8**, Co(II) **9** and Lu(III) **10** complexes were synthesized from the corresponding metal salts by the tetramerization of compound **5**. Compound **7** was prepared by the statistical condensation of **5** and 4,5-bis(hexylthio)phthalonitrile **6** with $CoCl_2 \cdot 6H_2O$ in dry dimethylformamide. The new compounds were characterized by FT-IR, UV/Vis, NMR and mass spectra. The electrochemical properties of the complexes were also investigated by cyclic voltammetry in non-aqueous medium. The effect of temperature on the dc conductivity and the impedance spectra of spin coated film of the compounds was investigated at temperatures between 295 and 433 K and in the frequency range 40–10^5 Hz. Thermally activated conductivity dependence on temperature was observed for all compounds.

Keywords: Phthalocyanine; Electrochemistry; Impedance spectra

1. Introduction

Phthalocyanines (Pcs) are well known colorants; besides their intense colour and efficient energy absorption, more remarkable properties have been discovered due to their 18 π-electron conjugated system. The past several years have seen an increasing interest in the chemistry of metallophthalocyanines (MPcs), since these compounds have been used as commercial dyes, optical and electrical materials, catalysts and models for naturally occurring macrocycles [1]. MPcs and their derivatives are semiconductive organic materials that have been used in various applications including chemical sensors, photoconductive agents, liquid crystals, non-linear optics, electrocatalysis and other photoelectronic devices [1]. Unsymmetrically substituted Pcs possess very interesting non-linear optical properties [2,3] and are important for Langmuir–Blodgett films [4–6] and photodynamic therapy of cancer [7]. Many Pcs are practically insoluble in common organic solvents and water. This minimizes their applications. However, the solubility of unsubstituted Pcs can be improved by introducing different kinds of substituents, such as crown ethers, alkyl, alkoxy and alkylthio, at the periphery of the Pcs [8]. The synthesis of soluble Pcs provides them with new optical, electronic,

* Corresponding author. Present address: Bilim Sokak, Kardesler Apt., No. 6/9, Erenköy, Istanbul, Turkey. Tel.: +90 216 359 01 30; fax: +90 216 386 08 24.
E-mail address: obekaroglu@gmail.com (Ö. Bekaroğlu).

0277-5387/$ - see front matter © 2007 Elsevier Ltd. All rights reserved.
doi:10.1016/j.poly.2007.08.015

redox and magnetic properties which could increase the field of possible applications [9,10]. The growing use of Pcs as advanced materials during the last decade has encouraged the synthesis of new materials [11] which differ in terms of the central metal ion and peripheral substituents [12].

The present paper reports for the first time the synthesis and characterisation of 4-nitro-2-octyloxyphenoxy substituted symmetrical and unsymmetrical MPcs. The electrical and electrochemical properties of the complexes are also presented.

2. Experimental

2.1. Synthesis and characterization

All chemicals used were of reagent grade. The solvents were dried, purified and stored over molecular sieves (4 Å). Compounds **2** and **6** were prepared by the literature methods [13,14]. Compound **1** was obtained from commercial suppliers. The progress of the reactions was monitored by TLC. Column chromotography was used for purification of the complexes. ^{1}H NMR spectra were determined with a Varian Unity Inova 500 MHz NMR spectrometer and a Varian Mercury-Vx 400 MHz NMR spectrometer. IR spectra were recorded as KBr discs in the range 400–4000 cm^{-1} on a Shimadzu FTIR-8300 infrared spectrometer. The electronic absorption spectra were measured in $CHCl_3$ with a Shimadzu UV-1601 UV/Vis spectrometer. Mass spectra were acquired on a Voyager-DE™ PRO MALDI-TOF mass spectrometer (Applied Biosystems, USA) equipped with a nitrogen UV-Laser operating at 337 nm. Spectra were recorded both in linear and reflectron modes with an average of 50 and 100 shots for linear and reflectron modes, respectively. A α-cyano-4-hydroxycinnamic acid (CHCA) MALDI matrix was used and prepared in chloroform at a concentration of 20 mg/mL for symmetrical Pcs **8** and **9**. A 3-indole acrylic acid (IAA) MALDI matrix was used for the unsymmetrical Pc **7**. The positive ion and linear mode spectrum of complex **10** could be obtained only in dithranol matrix. MALDI samples were prepared by mixing sample solutions (4 mg/mL) with the matrix solution (1:10 v/v) in a 0.5 mL eppendorf® microtube. Finally 1 μl of this mixture was deposited on the sample plate, dried at room temperature and then analyzed.

2.1.1. 3,4-Bis(3,4-dicyanophenoxy)nitrobenzene (*3*) and 4-(3,4-dicyanophenoxy)-3-hydroxynitrobenzene (*4*)

About 2 g (12.90 mmol) of **1**, 4.47 g (25.80 mmol) of **2** and 5.48 g (39.70 mmol) of K_2CO_3 in dry dimethylsulfoxide (DMSO) (30 ml) were stirred at 78–80 °C for 24 h under an argon atmosphere. Then, the reaction mixture was poured into water. The precipitate that formed was filtered, washed with cold water and dried in air. The crude compound **3** was chromatographed on a silica gel column with $CHCl_3$ as the eluent. After that, the separated filtrate was treated with hydrochloridic acid (10%) and the crude solid was filtered, washed with distilled water and ethanol. Column chromatography of this crude product on silica gel gave **4**. Products **3** and **4** were soluble in $CHCl_3$, dimethylformamide (DMF), DMSO and tetrahydrofurane (THF). Yield of **3**: 0.60 g (11%). M.p.: 193–196 °C. IR (γ_{max}/cm^{-1} KBr disc): 3083 (Ar–H), 2235 (–CN), 1588–1485 (–C=C–), 1246–1279 (Ar–O–C), 1569–1350 (–NO_2). ^{1}H NMR (δ_H ppm, 400 MHz, DMSO): 8.31 (d, $J = 2.73$, Ar–H), 8.26 (dd, $J = 2.73$, Ar–H), 8.20 (d, $J = 8.58$, Ar–H), 8.10 (d, $J = 8.58$, Ar–H), 8.06 (d, $J = 8.97$, Ar–H), 7.90 (d, $J = 2.34$, Ar–H), 7.86 (d, $J = 2.73$, Ar–H), 7.68 (dd, $J = 2.34$, Ar–H). Yield of **4**: 3.2 g (88%). M.p.: 213–215 °C. IR (γ_{max}/cm^{-1} KBr disc): 3037–3082 (Ar–H), 2223 (–CN), 1490–1598 (–C=C–), 1265–1136 (Ar–O–C), 1332–1525 (–NO_2), 3276 (Ar–OH). ^{1}H NMR (δ_H ppm, 500 MHz, DMSO): 8.14 (dd, $J = 2.44$, Ar–H), 8.09 (d, $J = 2.44$, Ar–H), 8.07 (d, $J = 8.97$, Ar–H), 7.79 (d, $J = 2.93$, Ar–H), 7.40 (dd, $J = 2.45$, Ar–H), 7.20 (d, $J = 8.79$, Ar–H), 11.6 (s, br, Ar–O–H). D_2O Exc-NMR (δ_H ppm, 500 MHz, DMSO): 8.12 (dd, $J = 2.44$, Ar–H), 8.09 (d, $J = 2.93$, Ar–H), 8.04 (d, $J = 8.79$, Ar–H), 7.72 (d, $J = 2.44$, Ar–H), 7.38 (dd, $J = 2.93$, Ar–H), 7.18 (d, $J = 9.28$, Ar–H).

2.1.2. Preparation of 4-(4-nitro-2-(octyloxy)phenoxy)phthalonitrile (*5*)

About 0.282 g (1 mmol) of **4**, 0.193 g (1 mmol) of 1-bromooctane, 0.278 g (2 mmol) of anhydrous K_2CO_3 and tetrabutylammonium bromide in dry acetonitrile (40 ml) were stirred at 80–85 °C for 48 h under an argon atmosphere. The mixture was cooled and evaporated to dryness. The product was treated with glacial-acetic acid and then flushed several times with water until the filtrate was neutral. After that it was extracted with CH_2Cl_2. Finally, pure **5** was obtained by chromatography with silica gel using $CHCl_3$. Product **5** was soluble in $CHCl_3$, CH_2Cl_2, DMF, DMSO and THF. Yield: 0.30 g (76%). M.p.: 88–92 °C (Scheme 1). IR (γ_{max}/cm^{-1} KBr disc): 3082 (Ar–H), 2234 (–CN), 1484–1606 (–C=C–), 1292–1246 (Ar–O–C), 1347 and 1512 (–NO_2), 2847–2932 (–CH_2–, –CH_3). ^{1}H NMR (δ_H ppm, 400 MHz, $CDCl_3$): 8.23 (dd, $J = 2.73$, Ar–H), 8.08 (d, $J = 2.73$, Ar–H), 7.73 (d, $J = 8.68$, Ar–H), 7.21 (dd, $J = 2.73$, Ar–H), 7.18 (d, $J = 2.34$, Ar–H), 7.10 (d, $J = 9.36$, Ar–H), 4.05 (t, $J = 6.24$, –OCH_2), 1.40 (m, –CH_2–), 0.90 (t, $J = 7.02$, –CH_3).

2.1.3. 2-[4-Nitro-2-(octyloxy)phenoxy]-9,10,16,17,23,24-hexakis(hexylthio)phthalocyaninato cobalt(II) (*7*)

Compounds **5** (0.150 g, 0.382 mmol) and **6** (0.412 g, 1.145 mmol) were dissolved in dry DMF (2–3 ml) in a tube. $CoCl_2 \cdot 6H_2O$ (90.44 mg, 0.382 mmol) was added to this solution. The mixture was heated and stirred at 160–170 °C for 24 h under nitrogen atmosphere to give an unsymmetrical substituted Pc (Scheme 1). After being cooled, the reaction mixture was poured into

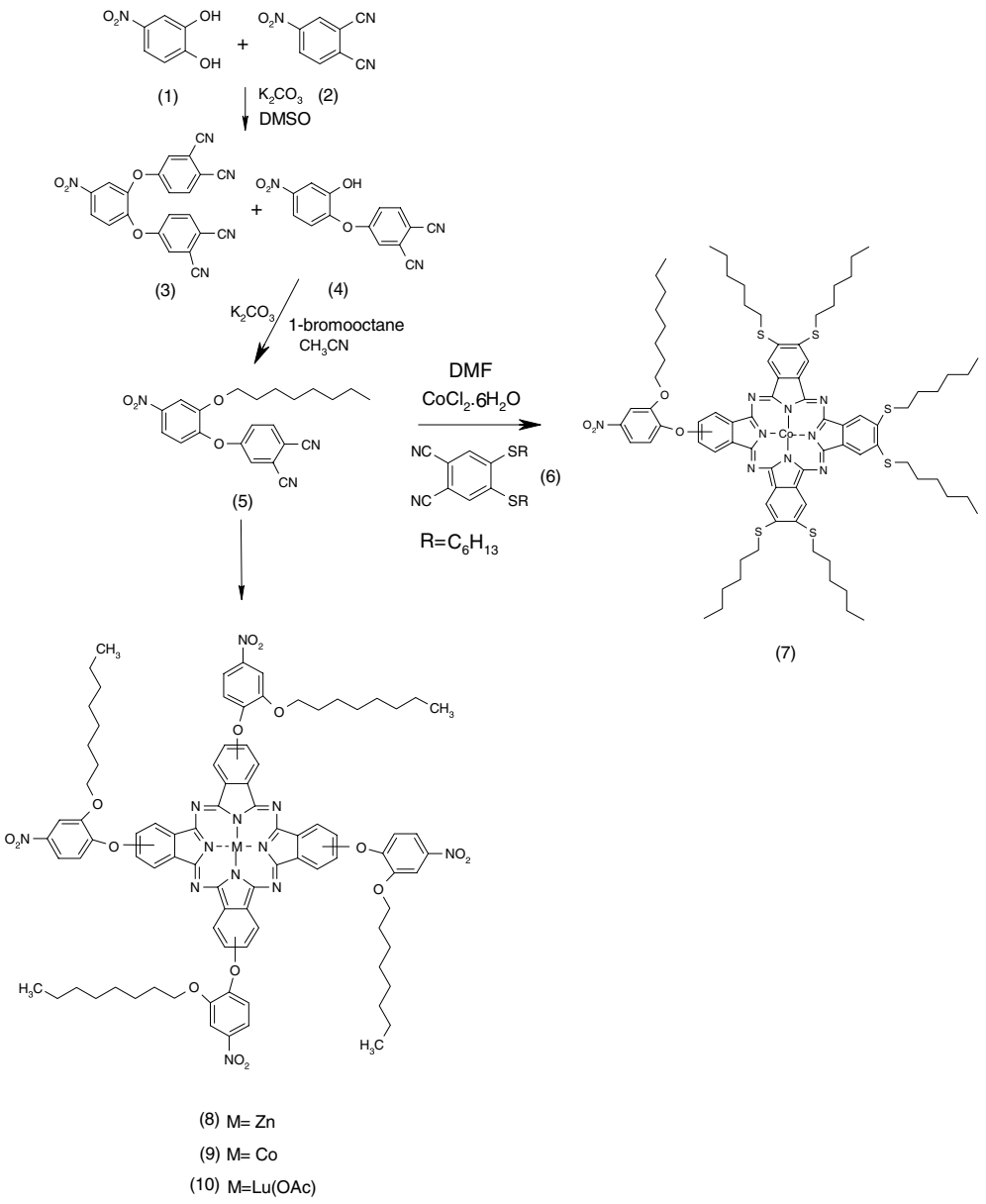

Scheme 1. Summary of the synthesis of compounds **3**–**10**.

50 ml of ethanol and the dark green precipitate that formed was separated by centrifugation. The crude Pc mixture was washed with cold acetic acid, water, ethanol and methanol, and then dried in a vacuum. The purification of that aimed Pc **7** was carried out on a silica gel column with a $CHCl_3$:hexane system, changing from 10/1 to 10/2 (v/v). Compound **7** is soluble in chloroform, dichloromethane, ethyl acetate, hexane, DMF, THF and DMSO. Yield of **7**: 0.12 g (20.50%). M.p.: >300 °C. IR (γ_{max}/cm^{-1} KBr disc): 3050 (Ar–H), 1411–1595 (–C=C–), 1222–1274 (Ar–O–C), 1377 and 1517 (–NO_2), 2860–2929 (–CH_2–, –CH_3), 1072–1124 (C–S). UV–Vis λ_{max} ($CHCl_3$) (log ε/dm^{-3} mol^{-1} cm^{-1}): 697(5.4739), 629(5.0012), 424 (4.7700), 327(5.4681). MS(MALDI-TOF): *m*/*z* 1533 Da mass ($M+H^+$) and $(M-32)^+$.

*2.1.4. 2,10,16,24-Tetrakis-[4-nitro-2-(octyloxy)phenoxy]-phthalocyaninatozinc(II) (**8**)*

A mixture of compound **5** (0.168 g, 0.427 mmol), anhydrous zinc acetate (0.094 g, 0.427 mmol) and DMF (3–4 ml) was heated and stirred at 180 °C for 6 h under nitrogen atmosphere. After cooling to room temperature, methanol (5 ml) was added in order to precipitate the product. The blue product was filtered off and then washed several times, first with methanol, then with acetonitrile and acetone. The crude product was isolated by silica gel column chromatography with chloroform as the eluent. This product is soluble in $CHCl_3$, DMSO, DMF and THF. Yield: 0.020 g (11.50%). M.p.: >300 °C. IR (γ_{max}/cm^{-1} KBr disc): 3040 (Ar–H), 1514–1650 (–C=C–), 1222–1282 (Ar–O–C), 1340 and 1558 (–NO_2), 2854–2921 (–CH_2–, –CH_3). UV–Vis λ_{max} ($CHCl_3$) (log ε/dm^{-3} mol^{-1} cm^{-1}): 679 (4.16),

611 (3.47), 342 (3.98). ^{1}H NMR (δ_H ppm, 400 MHz, $CDCl_3$): 8.10 (dd, $J = 2.73$, Ar–H), 7.98 (d, $J = 2.73$, Ar–H), 7.72 (d, $J = 8.19$, Ar–H), 7.60 (dd, $J = 3.12$, Ar–H), 7.12 (d, $J = 2$, Ar–H), 6.98 (d, $J = 8.97$, Ar–H), 4.12 (t, $J = 5.86$, –OCH_2), 3.95 (t, $J = 6.44$, –CH_3), 1.25 (m, $(–CH_2)_6$). MS (MALDI-TOF): m/z 1638.0019 ($M+H^+$).

2.1.5. 2,10,16,24-Tetrakis-[4-nitro-2-(octyloxy)phenoxy]-phthalocyaninatocobalt(II) (9)

A mixture of compound **5** (0.150 g, 0.382 mmol), 90.440 mg (0.3816 mmol) $CoCl_2$ and absolute ethylene glycol (4–5 ml) was heated and stirred at 160 °C for 22 h under nitrogen atmosphere. After cooling to room temperature, the reaction mixture was treated with ethanol to precipitate the dark-blue product, which was then filtered. This product is soluble in $CHCl_3$ and THF, and partially in CH_2Cl_2 and DMF (Scheme 1). Yield 19.5 mg (12.53%). M.p.: >300 °C. IR (γ_{max}/cm^{-1} KBr disc): 3082 (Ar–H), 1467–1600 (–C=C–), 1222–1282 (Ar–O–C), 1340–1508 (–NO_2), 2854–2921 (–CH_2–, –CH_3). UV–Vis λ_{max} ($CHCl_3$) (log ε/dm^{-3} mol^{-1} cm^{-1}): 671 (4.24), 605 (3.63), 327 (4.10); MS (MALDI-TOF): m/z 1633.0136 ($M+H^+$).

2.1.6. 2,10,16,24-Tetrakis-[4-nitro-2-(octyloxy)phenoxy]-phthalocyaninato lutetium(III) acetate (10)

A mixture of $Lu(OAc)_3 \cdot nH_2O$ (0.023 g, 0.065 mmol), **5** (0.400 g, 1.018 mmol) and DBU (1.130 mg, 0.009128 mmol) in pentanol (2.5 ml) was refluxed under nitrogen atmosphere at 175–180 °C for 20 h. The dark green mixture was cooled to room temperature and then was washed with water, acetonitrile, ethanol, methanol and acetone, and then dried in vacuum. Compound **10** is soluble in acetic acid and THF, and partially in DMF and DMSO. Yield 0.155 g (36.70%). M.p.: >300 °C (Scheme 1). IR(γ_{max}/cm^{-1} KBr disc); 3066 (Ar–H), 1469–1666 (–C=C–), 1213–1276 (Ar–O–C), 1334 and 1506 (–NO_2), 2858–2925 (–CH_2–, –CH_3). UV–Vis λ_{max} (DMF) (log ε/dm^{-3} mol^{-1} cm^{-1}): 685 (4.8140), 618 (4.3802), 334 (5.0307). MS (MALDI-TOF): m/z 1808 ($M+H^+$).

2.2. Electrochemistry

The cyclic voltammetry, differential pulse voltammetry and controlled potential chronocoulometry (CPC) measurements were carried out with a Princeton Applied Research Model Versostat II potentiostat/galvanostat controlled by an external PC and utilizing a three-electrode configuration at 25 °C. The working electrode was a Pt plate with a surface area of 0.10 cm^2. The surface of the working electrode was polished with a H_2O suspension of Al_2O_3 before each run. The last polishing was done with a particle size of 50 nm. A Pt wire served as the counter electrode. A saturated calomel electrode (SCE) was employed as the reference electrode and was separated from the bulk of the solution by a double bridge. Electrochemical grade tetrabutylammonium perchlorate (TBAP) in extra pure DMSO was employed as the supporting electrolyte at a concentration of 0.10 mol dm^{-3}. High purity N_2 was used for deoxygenating the solution for at least 20 min prior to each run and to maintain a nitrogen blanket during the measurements. For CPC studies, a Pt gauze working electrode (10.5 cm^2 surface area), a Pt wire counter electrode separated by a glass bridge, and an SCE as a reference electrode were used.

2.3. Electrical measurements

For the electrical and impedance measurements, an interdigital comb structure with a 100 μm gap on glass substrate was used. Thin films of compounds were obtained by the spin-coating method. The substrate temperature was kept constant at 290 K during deposition of the materials over the electrodes. Dc conductivity and impedance spectral measurements were performed between 295 and 433 K using a Keithley 617 electrometer. Ac conductivity and impedance measurements were carried out with a Keithley 3330 LCZ meter in the frequency range 40–10^5 Hz, in the temperature range 295–433 K.

3. Results and discussion

3.1. Synthesis and characterization

Starting from **1** and **2**, a general synthetic route for the synthesis of new symmetrical and unsymmetrical Pcs is given in Scheme 1. Compounds **3** and **4** were obtained by base-catalyzed nucleophilic aromatic nitro displacement, in 10% and 88% yield, respectively. The reaction was carried out in a single step synthesis by using K_2CO_3 as the nitro-displacing base at 78–80 °C in dry DMSO under an argon atmosphere. Starting from **4** and 1-bromooctane, the general alkylation reaction gave **5** in the presence of K_2CO_3 at 80–85 °C for 48 h under an argon atmosphere in 75% yield. The symmetrical MPcs **8**, **9** and **10** were obtained from the dicyano derivative **5** and the corresponding metal salts ($Zn(OAc)_2$, $CoCl_2$, $Lu(OAc)_3 \cdot nH_2O$) in suitable anhydrous solvents under reflux in a sealed tube, in 12%, 13% and 36.7% yields, respectively. The high boiling solvents of choice for these reactions were DMF for Zn(II)Pc **8**, ethylene glycol for Co(II)Pc **9** and pentanol for Lu(III)(OAc)Pc **10**. These symmetrical MPcs were isolated by column chromatography on silica gel using $CHCl_3$ as the eluent. The unsymmetrical Co(II)Pc **7** was synthesized by $CoCl_2$-mediated statistical condensation of a 3:1 molar ratio of **5** and **6** in anhydrous DMF under reflux for 24 h. Product **7** was separated by column chromatography on silica gel using different $CHCl_3$:hexane solvent systems, changing from 10/1 to 10/2 (v/v), as the eluent. All the Pcs **7**, **8**, **9** and **10** show good solubility in common organic solvents such as chloroform, dichloromethane and tetrahydrofuran. The spectroscopic characterization of the newly synthesized compounds included ^{1}H NMR, IR, UV/Vis and mass spectral investigations, and the results are in accordance with the proposed structures.

The IR spectra of **3**, **4** and **5** indicate the presence of –C≡N groups by the intense stretching bands at 2235, 2223 and 2234 cm^{-1}, respectively. The IR spectra of **3**, **4** and **5** exhibit characteristic frequencies at 3037–3083 (Ar–H), 1485–1598 (–C=C–), 1136–1292 (Ar–O–C), 1332 and 1569 ($–NO_2$) cm^{-1}. The IR spectra of **3**, **4** and **5** are very similar, except those of **4** (Ar–OH) with vibrations at 3276 cm^{-1} and of **5** ($–CH_2–$, $–CH_3$) with vibrations at 2847–2932 cm^{-1}. Cyclotetramerization of dinitriles **5** to Pcs **7**, **8**, **9** and **10** was confirmed by the disappearance of the sharp –C≡N vibration at 2234 cm^{-1}. The IR spectra of the symmetrical Pcs **8**, **9** and **10** and the unsymmetrical Pc **7** are very similar, except for the C–S vibrations at 1072–1124 cm^{-1}. The IR spectra of **8**, **9** and **10** exhibit characteristic frequencies at 3230–3066 (Ar–H), 1467–1650 (–C=C–), 1213–1282 (Ar–O–C), 1334–1558 ($–NO_2$) and 2854–2925 ($–CH_2–$, $–CH_3$) cm^{-1}.

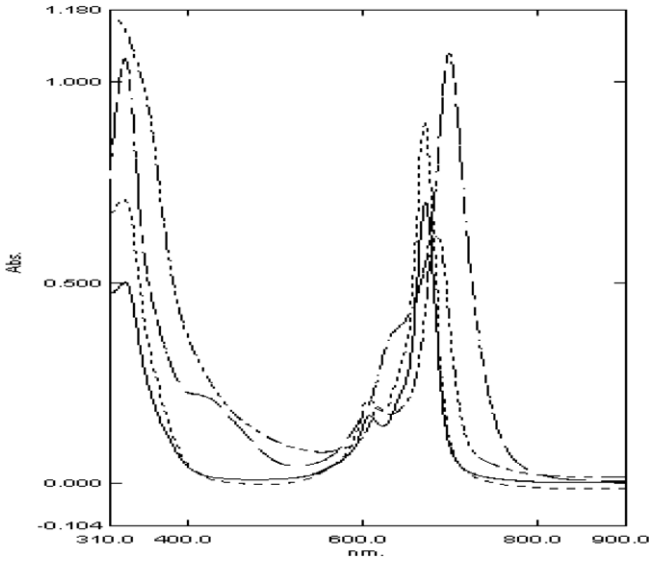

Fig. 1. UV–Vis spectra of **7**, **8**, **9** and **10** (– – – **7**, . . . **8**, — **9**, - - - **10**) (**7**, **8**, **9** in $CHCl_3$, **10** in DMF).

In the ^1H NMR spectra of **3**, **4** and **5**, the aromatic protons of the compounds appear in the low field region around 8.32–7.12 ppm. The octyl protons of **5** are observed between 0.86 and 4.07 ppm. The hydroxy proton of **4** appears at a lower field around 11.6 ppm. In the D_2O exchanged NMR spectrum of **4** this assignment was confirmed by the disappearance of the sharp hydroxy proton peak at 11.6 ppm. The ^1H NMR spectra of Zn(II)Pc **8** are almost identical. The aromatic protons of **8** appear in the low field region around 7.00–8.12 ppm. The octyl protons are observed in the range 0.70–4.14 ppm. The ^1H NMR spectra of the unsymmetrical Co(II)Pc, symmetrical Co(II)Pc and Lu(III)(OAc)Pc could not be determined because of the presence of paramagnetic cobalt and lutetium atoms.

Pcs **7**, **8**, **9** and **10** show typical electronic spectra with two strong absorption regions, one of them in the UV region at about 300–400 nm (B band) arising from the deeper π-levels → LUMO transition and the other in the visible part of the spectrum around 600–700 nm (Q band) attributed to the $\pi \rightarrow \pi^*$ transition from the highest occupied molecular orbital (HOMO) to the lowest unoccupied molecular orbital (LUMO) of the Pc^{2-}ring. Spectra of the symmetrical Zn(II) and Co(II) phthalocyanines **8** and **9** in chloroform are very similar, with intense Q bands at 679 and 671 nm due to a single $\pi \rightarrow \pi^*$ transition with shoulders at 611 and 605 nm and B bands at 342 and 327 nm, respectively. The splitting of the Q band of both compounds shows aggregation. The spectrum of **7** in chloroform shows a characteristic Q band absorption around 697 nm (with a shoulder at 629 nm) and B band absorptions around 424 and 327 nm. The spectrum of **10** in DMF indicates a Q band absorption around 685 nm and a B band absorption around 334 nm (Fig. 1). In the spectra of both compounds, besides the splitting of the Q band, a very strong of soret band indicates strong aggregation of both compounds [15].

Positive ion MALDI-MS spectra of **7**, **8**, **9** and **10** are given in Figs. 2–5, respectively. Many different MALDI matrices were tried to find an intense molecular ion peak

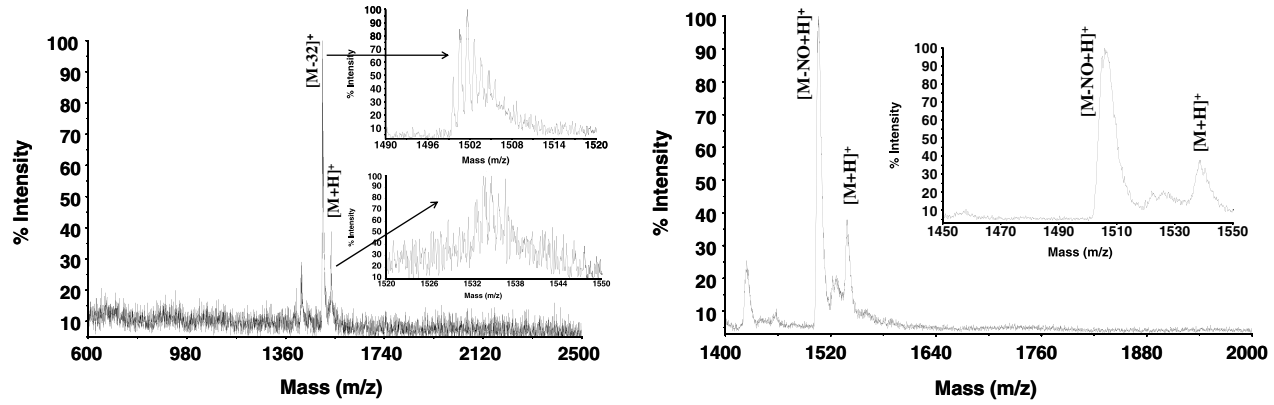

Fig. 2. MALDI-MS spectrum of the unsymmetrical Co(II)Pc **7** (left: linear mode; right: reflectron mode).

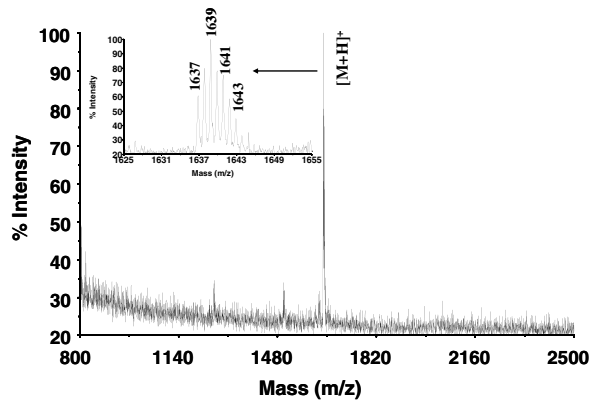

Fig. 3. MALDI-MS spectrum of the symmetrical Zn(II)Pc **8**.

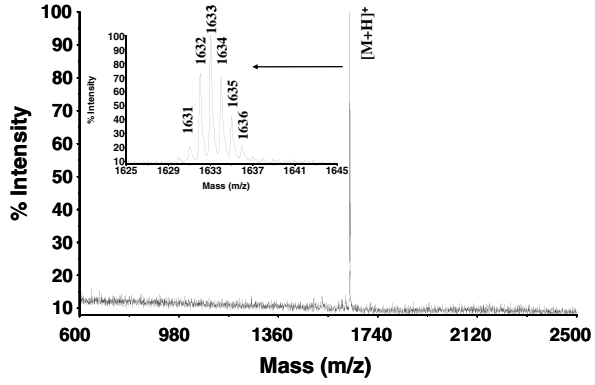

Fig. 4. MALDI-MS spectrum of the symmetrical Co(II)Pc **9**.

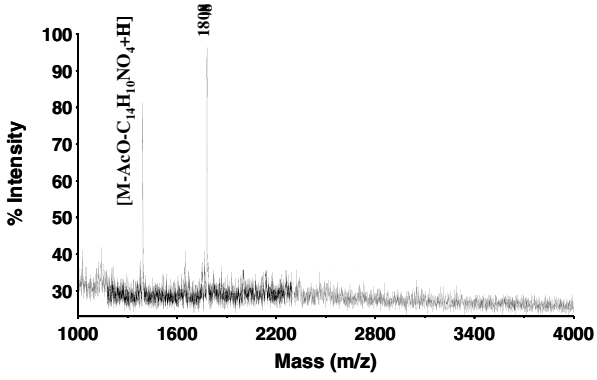

Fig. 5. MALDI-MS spectrum of the symmetrical Lu(III)(AcO)Pc **10**.

and low fragmentation under the MALDI-MS conditions for the complexes.

For complex **7**, 3-indole acrylic acid MALDI matrix yielded the best MALDI-MS spectrum. The peak group representing the protonated molecular ion of the complex was observed, starting with 1533 Da mass and finishing with 1537 Da, following each other by 1 Da mass differences. The intensity of the protonated molecular ion peak was really low when the MALDI-MS spectrum was monitored by the laser shots higher than 20. Therefore, the MALDI-MS spectrum for this complex was accumulated using 10 laser shots so as not to give high fragmentation. In this case, however, the resolution was observed at very low values of about 2500. When the number of laser shots was chosen to be between 1 and 5, more intense spectra could be obtained but the resolution was really diminished this time. Because of all these reasons, the resolution and the intensity of the protonated molecular ion peak were optimized accumulating an average of 10 laser shots for this complex. On the protonated molecular ion peak, there is an isotopic distribution resulting from ^{13}C and the isotopes of cobalt. In the positive ion MALDI-MS spectrum of **7**, beside the protonated molecular ion peak, two peaks were observed, one at high and the other at low intensity. The intense peak is because of the fragmentation of the complex. At the end of this fragmentation, the leaving group was observed as O_2, having 32 Da mass. The O_2 leaving group results from NO_2 functional groups. The second fragment peak is due to side chain elimination ($C_8H_{17}O$ leaving). This pointed out that the complex was not more stable under the MALDI matrix conditions than under the laser energy, but the positive ion MALDI-MS spectra could be carried out by MALDI-MS.

α-Cyano-4-hydroxycinnamic acid MALDI matrix yielded the best MALDI-MS spectra for **8** and **9**. The peak group representing the protonated molecular ion of **8** was observed, starting with 1637 Da mass and finishing with 1644 Da, following each other by 1 Da mass differences. This type of mass distribution resulted from the isotopic mass distribution of carbon (mainly ^{13}C) and the isotopes of zinc and cobalt in the metal complexes. The experimentally obtained isotopic mass distribution of **9** overlapped with the theoretical isotopic mass distribution calculated using isotopes of carbon and cobalt. In the MALDI-MS spectrum of **8**, besides the protonated molecular ion peak, two peaks were observed with very low intensities. These peaks are due to side chain elimination (mainly $C_8H_{17}O$) and also the other whole side chain elimination. This pointed out that the complex was very stable under the MALDI matrix conditions and also under the laser energy. The peak group representing the protonated molecular ion of **9** was observed starting with 1631 Da mass and finishing with 1636 Da, following each other by 1 Da mass differences. In the MALDI-MS spectrum of **9**, besides the protonated molecular ion peak, no fragment ion was observed. This suggests that no leaving group was available for this complex and the complex is very stable under the MALDI matrix conditions and also under the laser energy.

The positive ion and linear mode spectra of **10** could be obtained only in dithranol matrix compared to the other novel MALDI matrices. The protonated molecular ion peak of the complex was observed at 1808 Da. Beside the protonated molecular ion peak, only one another peak was observed, representing the AcO (acetate) and $C_{14}H_{20}NO_4$ groups leaving from the protonated ion peak. Limited fragmentations showed that this complex has high stability under the laser firing and MALDI-MS conditions.

The protonated molecular ion peak mass showed that a lutetium complex containing a single ligand and acetate ion was synthesized instead of the sandwich type lutetium complex. From the clean spectrum, it could be noticed that the purity of the synthesized lutetium complex was very high.

3.2. Electrochemistry

The solution redox properties of the Pc complexes (**7**–**10**) were studied using cyclic voltammetry, differential pulse voltammetry and controlled potential chronocoulometry in DMSO with a platinum electrode. Complete electrolysis of each Pc solution at the working electrode at a suitable constant potential for each redox process was achieved, and the time integration of the electrolysis current was recorded with the controlled potential coulometry studies. The charge, Q, at the end of the electrolysis was calculated using the current–time response of the solution and *Faraday*'s law was used to estimate the number of electrons transferred. The number of electrons was found to be one for all the redox processes observed in this study. Voltammetric data and the assignment of the redox couples recorded for the complexes are listed in Table 1. Fig. 6 shows typical cyclic and differential pulse voltammograms of **9** in DMSO containing TBAP.

Complex **8** gives three one-electron reduction processes labelled as R_1 at −0.67 V, R_2 at −0.98 V and R_3 at −1.76 V, and a one-electron oxidation process labelled as O_1 at 0.85 V vs. SCE at 0.100 V s^{-1} scan rate (Table 1). Voltammetric studies revealed that the redox behaviours of **8** and **10** are very similar to each other and to the metal-free Pcs [16] (Table 1). This similarity suggests that

Table 1
The electrochemical data of the Pc complexes

Complex	Redox processes	$E^{a}_{1/2}$ (V vs. SCE)	ΔE^{b}_{p} (V)	I_{pa}/I^{c}_{pc}	$\Delta E^{d}_{1/2}$ (V)
8	R1	−0.67	0.070	0.96	1.52
	R2	−0.98	0.080	0.98	
	R3	−1.76	0.160	[e]	
	O1	0.85	0.060	[e]	
9	R1	−0.37	0.100	1.00	0.82
	R2	−1.28	0.080	0.96	
	O1	0.45	0.100	0.95	
7	R1	−0.40	0.080	0.97	0.88
	R2	−1.32	0.090	0.96	
	O1	0.48	0.090	0.98	
10	R1	−0.73	0.080	0.94	1.48
	R2	−1.03	0.090	1.00	
	R3	−1.82	0.120	[e]	
	O1	0.75	0.140	0.98	

[a] $E_{1/2} = (E_{pa} + E_{pc})/2$ at 0.100 V s^{-1}.
[b] $\Delta E_p = E_{pa} - E_{pc}$ at 0.100 V s^{-1}.
[c] I_{pa}/I_{pc} for reduction, I_{pc}/I_{pa} for oxidation processes at 0.100 V s^{-1}.
[d] $\Delta E_{1/2} = E_{1/2}$(first oxidation) − $E_{1/2}$(first reduction). This value reflects the HOMO–LUMO gap for **8** and **10**, but not **7** and **9**.
[e] ΔE_p could not be determined due to an ill-defined redox wave.

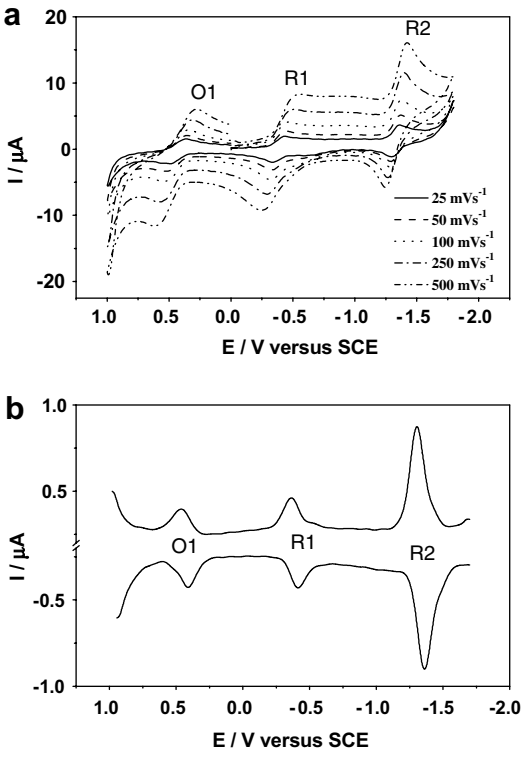

Fig. 6. Cyclic (a) and differential pulse (b) voltammograms of **9** in TBAP/DMSO.

all the one-electron redox processes of these complexes are Pc ring based. However, the redox potentials of **10** occur at potentials slightly more negative as compared to **8**. The shift in the potentials can be attributed to the difference in the polarizing effect of the metal ions. Reduction of the Pc ligand is associated with the position of the LUMO, whereas oxidation of the ligand is associated with the position of the HOMO. Thus the difference between the potentials of the first oxidation and the first reduction processes ($\Delta E_{1/2}$) reflects the HOMO–LUMO gap for metal free Pcs and it is closely related to the HOMO–LUMO gap in MPc species involving a redox inactive metal center. The $\Delta E_{1/2}$ values recorded for **8** and **10** in this study are in agreement with the values reported previously for the relevant Pcs involving a redox-inactive metal center [16]. The ratio of the anodic to the cathodic peak currents for the couples of **8** and **10** is close to unity, suggesting reversible redox processes. The anodic to cathodic peak separations (ΔE_p) changed from 0.070 to 0.140 V within the scan rates from 0.010 to 0.500 V s^{-1}(ΔE_p changed from 0.060 to 0.140 V for ferrocene), providing additional support for the reversible electron transfer. The peak currents increased linearly with the square root of the scan rates for scan rates ranging from 0.010 to 0.500 V s^{-1}, indicating purely diffusion-controlled behavior [17].

The redox potentials of **7** and **9** are considerably similar to each other, but highly different as compared to those of **8** and **10** (Table 1). Within the electrochemical window of TBAP/DMSO, compounds **7** and **9** undergo a reversible

one-electron oxidation and two reversible one-electron reductions with anodic to cathodic peak separations (ΔE_p) changing from 0.080 to 0.100 V within scan rates from 0.010 to 0.500 V s^{-1}. The peak currents increased linearly with the square root of the scan rates for scan rates ranging from 0.010 to 0.500 V s^{-1}, indicating purely diffusion-controlled behavior [17]. The difference in the voltammetric behaviour of these complexes as compared to those of **8** and **10** is due to the fact that metallo phthalocyanines, such as MnPc, CoPc and FePc, having a metal that possesses energy levels lying between the HOMO and the LUMO of the Pc ligand, in general exhibit redox processes centered on the metal [16,18–21]. Moreover, the electrochemistry of CoPc is dependent on the coordinating nature of the solvents. For CoPc complexes, the first oxidation and the first reduction processes occur on the metal center in polar coordinating solvents such as DMF and DMSO, whilst the first oxidation process occurs on the Pc ring in non-polar solvents such as DCM and THF. Therefore, the first reduction and the first oxidation processes of **7** and **9** could be assigned easily to the $[Co(II)Pc(-2)]/[Co(I)Pc(-2)]^-$ and $[Co(II)Pc(-2)]/[Co(III)Pc(-2)]^+$ redox couples and the second reduction process to the Pc ring as $[Co(I)Pc(-2)]^-/[Co(I)Pc(-3)]^{2-}$. The separation between the first oxidation and the first reduction potentials of the metal center for these Co(II) complexes (0.88 for **7** and 0.82 V for **9**) is comparable with the relevant values in the literature [15,17–20], and does not reflect the HOMO–LUMO gap. The small differences between the redox potentials of **7** and **9** can be attributed to the difference in peripheral substituents attached to the Pc core.

3.3. Electrical measurements

Arrhenius-type behavior is clearly observed from the temperature dependent conductivity measurements for all the compounds. A linear fit to $\sigma_{dc} = \sigma_0 \exp(-E_A/kT)$ is shown with different correlation coefficients. The electrical parameters corresponding to the studied compounds are shown in Table 2.

The frequency dependence of the ac conductivity, $\sigma_{ac}(\omega)$, for different values of temperatures between 295 and 433 K was investigated for all samples. The frequency dependence of the ac conductivity is shown in Fig. 7 for all compounds as a plot of $\ln \sigma_{ac}$ versus $\ln \omega$ at 373 K. The general observed frequency dependence of the ac conductivity in disordered systems, such as phthalocyanine, is that the ac conductivity obeys an empirical power law of the form $\sigma_{ac}(\omega) = A(T)\omega^s$, where $A(T)$ and s are temperature dependent parameters. To explain this type of frequency dependence of the ac conduction, two models have been used. According to the first model, which is known as the quantum mechanical tunnelling model (QMT), the conduction occurs by means of thermally assisted Quantum Mechanical Tunnelling. The other model, which is known as the Correlated Barrier Hopping (CBH) model, is based on the concept of charged defects and in this bipolarons hop between two charged defect states D^+ and D^- over the barrier separating them. In these two models, the frequency exponent s is found to have two different trends with temperature and frequency [22]. The values of the frequency exponent s were calculated from the slope of the measured $\ln \sigma_{ac}$ versus $\ln \omega$ graphs. Our results showed that s is definitely a function of temperature for all the compounds and shows a general tendency to decrease with increasing temperature. This is in agreement with the prediction of the CBH model.

Table 2
The electrical parameters of the Pc complexes

Samples	$\sigma_{290\,K}$ (Ω^{-1} cm^{-1})	E_A (eV)	$\sigma_{433\,K}$ (Ω^{-1} cm^{-1})
7	8.76×10^{-9}	0.81	1.41×10^{-4}
8	1.82×10^{-9}	0.79	1.07×10^{-4}
9	2.959×10^{-8}	0.70	1.84×10^{-4}
10	3.16×10^{-7}	0.72	2.1×10^{-4}

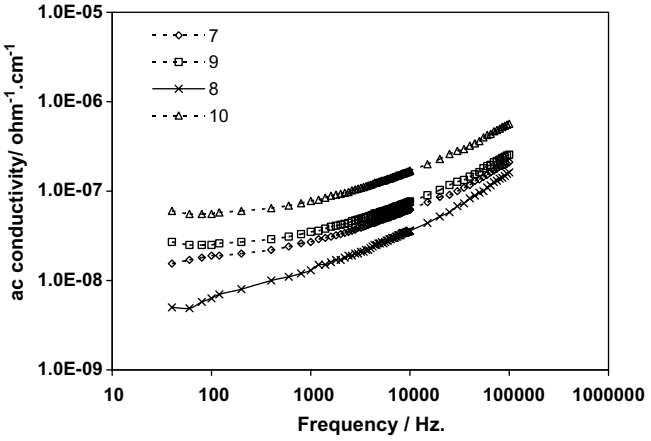

Fig. 7. The variation of the ac conductivity with frequency at 373 K.

To get more detailed information about the electrical properties of the compounds, impedance spectral measurements in the frequency range 40–10^5 Hz were also carried out on a spin coated film of the compounds. The measured impedance spectra, when plotted in a complex plane plot,

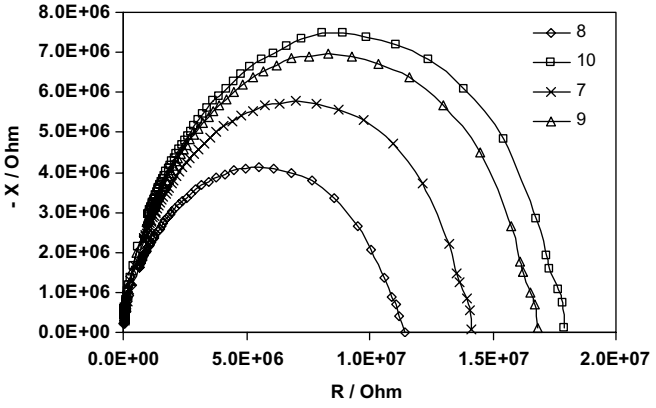

Fig. 8. Impedance spectra of the Pc films at 400 K.

appear in the form of a succession of semi-circles representing the contributions to the electrical properties due to bulk material, grain boundary effect and interfacial polarization phenomena. So, the impedance spectra technique enables us to separate the effects due to each component. At low temperatures, the impedance spectra consist of a quasi-vertical line. The existence of semicircular shaped curves in the Nyquist plot means that the impedance becomes capacitive even at relatively high frequencies. The effect of temperature on the impedance spectra of the films becomes clearly visible with a rise in the temperature. On the complex plane plot at high temperatures, only depressed semicircles with different radii were observed at higher temperatures, indicating deviation from the Debye dispersion relation (Fig. 8). In the case of a depressed semi-circle in the impedance spectra, the relaxation time is considered as a distribution of values, rather than a single relaxation time.

Acknowledgements

This work was supported in part by The Turkish Academy of Sciences (TUBA), TÜBİTAK (Project No. 106T326), The Research Fund of Marmara University (SCIENCE-YLS-290506-0124) and The State Planning Organization (DPT-2003K120810).

References

[1] C.C. Leznoff, A.B.P. Lever (Eds.), Phthalocyanines, Properties and Applications, vols. 1–4, VCH, New York, 1989, 1992, 1993, 1996.
[2] G. De la Torre, P. Vazquez, F. Agullo-Lopez, T. Torres, J. Mater. Chem. 8 (1998) 1671.
[3] N.B. McKeown, Phthalocyanine Materials, Cambridge University Press, Cambridge, 1998.
[4] M.J. Cook, M.F. Daniel, K.J. Harrison, N.B. McKeown, A.J. Thomson, J. Chem. Soc., Chem. Commun. (1987) 1148.
[5] M.A. Diaz-Garcia, J.M. Cabrera, F. Agulló-López, Appl. Phys. Lett. 3 (1996) 69.
[6] H. Schultz, H. Lehmann, M. Rein, M. Hanack, Struct. Bond. 74 (1991) 41.
[7] I. Rosenthal, Photochem. Photobiol. 53 (1991) 859.
[8] R. Zhou, F. Josse, W. Göpel, Z.Z. Özturk, Ö. Bekaroglu, Appl. Organomet. Chem. 10 (1996).
[9] M.J. Cook, J. Mater. Chem. 6 (1996) 677.
[10] J.C. Swarts, E.H.G. Langner, N. Kroeide-Hove, M.J. Cook, J. Mater. Chem. 11 (2001) 434.
[11] S. Abdurrahmanoglu, A. Altindal, A.R. Özkaya, M. Bulut, O. Bekaroglu, Chem. Commun. (2004) 2096.
[12] T. Ceyhan, A. Altindal, A.R. Ozkaya, M.K. Erbil, B. Salih, Ö. Bekaroglu, Chem. Commun. (2006) 320.
[13] J.G. Young, W.J. Onyebuagu, Org. Chem. 55 (1990) 2155.
[14] A.G. Gürek, Ö. Bekaroğlu, J. Chem. Soc., Dalton Trans. (1994) 1419.
[15] N. Kobayashi, Y. Niskiyama, T. Ohya, M. Sato, J. Chem. Soc., Chem. Commun. (1987) 390.
[16] A.B.P. Lever, E.R. Milaeva, G. Speier, in: C.C. Leznoff, A.B.P. Lever (Eds.), Phthalocyanines: Properties and Applications, vol. 3, VCH Publishers, New York, 1993, pp. 1–63.
[17] A.J. Bard, L.R. Faulkner, Electrochemical Methods: Fundamentals and Applications, 2nd ed., Wiley, New York, 2001.
[18] M. Özer, A. Altindal, A.R. Özkaya, M. Bulut, Ö. Bekaroglu, Polyhedron 25 (2006) 3593.
[19] A.R. Özkaya, E. Hamuryudan, Z.A. Bayır, Ö. Bekaroglu, J. Porphyr. Phthalocya. 4 (2000) 689.
[20] M. Kandaz, A.R. Özkaya, Ö. Bekaroğlu, Monatsh. Chem. 132 (2001) 1013.
[21] A. Koca, H.A. Dinçer, H. Çerlek, A. Gül, M.B. Koçak, Electrochim. Acta 52 (2006) 1199.
[22] S.R. Elliot, Adv. Phys. 36 (1987) 135.